Inorg. Chem. **1994,** *33,* 6140−6147

Synthesis, Structure, and Solution Equilibria of Diamagnetic and Paramagnetic Azooximates of Bivalent Platinum. Geometrical Change Associated with Ligand-Based Electroprotic Reactions

Chandan Kumar Pal, Surajit Chattopadhyay, Chittaranjan Sinha, and Animesh Chakravorty*

Department of Inorganic Chemistry, Indian Association for the Cultivation of Science,
Calcutta 700032, India

Received May 4, 1994[⊗]

(Phenylazo)benzaldoxime, PhN=NC(Ph)=NOH (Hpbo), reacts with K_2PtCl_4 in alkaline media affording *trans*-$Pt(pbo)_2$. One-electron−one-proton electroprotic transformation converts it to a cis complex isolated as the dimer [*cis*-Pt(pbo)(Hpbo)]$_2$. Both complexes are diamagnetic in the solid state. In *trans*-$Pt(pbo)_2$, the PtN_4 coordination sphere is planar, the metal atom being a center of inversion. In the cis dimer one monomer is stacked on the other such that the Pt⋯Pt (3.235(1) Å) midpoint is a center of inversion. Each metal atom is displaced by 0.088 Å from its N_4 plane toward its neighbor. Unsymmetrical and nearly linear $O\cdots H-O$ bridging is present within each monomer. In dichloromethane solution, the equilibrium dimer ($s = 0$) $\rightleftharpoons$ 2 monomer ($s = {}^1/_2$) exists. The paramagnetic monomer is EPR-active ($g = 1.987$). The intensity of the EPR-signal as well as the paramagnetic moment progressively diminishes with decreasing temperature due to the shift of the equilibrium to the left. The ΔH and ΔS values associated with dissociation are 8.3(±2) kcal mol^{-1} and 23.5(5) cal mol^{-1} K^{-1}, respectively. EHMO studies have revealed that the unpaired electron in the cis monomer (idealized point group C_s) resides in an azoimine orbital (3A″) with a large azo-π^* contribution. The EPR spectrum is consistent with this. The cis monomer is essentially a stable free radical. In dimer (C_i) formation 3A″−3A″ and $d_{z^2}-d_{z^2}$ interactions contribute significantly to binding. The doubly occupied $6A_g$ HOMO of the dimer corresponds to the bonding 3A″−3A″ combination. Accordingly the average N=N length in the cis dimer (1.31 Å) is longer than that in the trans complex (1.28 Å) in which the azo-π^* orbitals are empty and constitute the LUMO. The cis monomer displays quasireversible one-electron oxidation ($E_{1/2}$, 0.52 V vs SCE) and in presence of NEt_3 the oxidized complex is deprotonated affording the sterically favorable *trans*-$Pt(pbo)_2$. The latter is reconverted to the $O\cdots H-O$ stabilized cis complex via one-electron reduction ($E_{1/2}$, −0.28 V) and proton addition. In this remarkable family, metal geometry is controlled by electroprotic transfer at ligand sites: azo-π^* (electron transfer) and oximato oxygen (proton transfer). Crystal data for the complexes are as follows. *trans*-$Pt(pbo)_2$: crystal system monoclinic; space group $P2_1/n$; $a = 5.646(4)$ Å, $b = 10.784(7)$ Å, $c = 18.367(14)$ Å; $\beta = 98.11(5)°$; $V = 1107(1)$ Å^3; $Z = 2$; $R = 2.74\%$; $R_W = 3.20\%$. [*cis*-Pt(pbo)(Hpbo)]$_2$: crystal system monoclinic; space group $C2/c$; $a = 25.183(8)$ Å, $b = 8.849(4)$ Å, $c = 20.839(8)$ Å; $\beta = 90.09(3)°$; $V = 4644(3)$ Å^3; $Z = 4$; $R = 2.42\%$; $R_W = 2.90\%$.

Introduction

There is abiding chemical interest in metal chelates of unsaturated ligands that are themselves potential sites of facile electron transfer.[1] Notable examples are the dithiolenes,[2] dioxolenes,[3−5] and diimines.[6−12] Herein we introduce the azooxime chelate system[13−15] **1** as a potential electroproticacceptor i.e., acceptor of both an electron and a proton.[16] The specific case disclosed is that of a platinum(II) bis chelate which upon such acceptance undergoes spontaneous geometrical rearrangement, the product being observable in both monomeric and dimeric forms. Synthetic, structural, and thermodynamic aspects of this remarkable platinum system are examined in this work. The findings have necessitated a reevaluation of certain earlier results.[17]

Results and Discussion

A. Synthesis. The ligand used in the present work is (phenylazo)benzaldoxime PhN=NC(Ph)=NOH, abbreviated Hpbo. Aqueous alkaline solutions of Hpbo react smoothly, eq

---

[⊗] Abstract published in *Advance ACS Abstracts,* November 1, 1994.

(1) Ghosh, B. K.; Chakravorty, A. *Coord. Chem. Rev.* **1989**, *95*, 129.

(2) (a) Burns, R. P.; McAuliffe, C. A. *Adv. Inorg. Chem. Radiochem.* **1979**, *22*, 303. (b) Eisenberg, R. *Inorg. Chem.* **1970**, *12*, 295. (c) McCleverty, J. A. *Prog. Inorg. Chem.* **1968**, *10*, 49.

(3) (a) Pierpont, C. G.; Buchanan, R. M. *Coord. Chem. Rev.* **1981**, *38*, 45. (b) Bhattacharya, S.; Boone, S. R.; Fox, G. A.; Pierpont, C. G. *J. Am. Chem. Soc.* **1990**, *112*, 1088. (c) Bhattacharya, S.; Pierpont, C. G. *Inorg. Chem.* **1991**, *30*, 1511 and 2906. Bhattacharya, S.; Pierpont, C. G. *Inorg. Chem.* **1992**, *31*, 35 and references therein.

(4) (a) Lever, A. B. P.; Auburn, P. R.; Dodsworth, E. S.; Haga, M.; Liu, W.; Melink, M.; Nevin, W. A. *J. Am. Chem. Soc.* **1988**, *110*, 8076. (b) Masui, H.; Lever, A. B. P.; Auburn, P. R. *Inorg. Chem.* **1991**, *30*, 2402 and references therein.

(5) (a) Bag, N.; Paramanik, A.; Lahiri, G. K.; Chakravorty, A. *Inorg. Chem.* **1992**, *31*, 40. (b) Bag, N.; Lahiri, G. K.; Basu, P.; Chakravorty, A. *J. Chem. Soc., Dalton Trans.* **1993**, 113.

(6) Van Koten, G.; Vrieze, K. *Adv. Organomet. Chem.* **1982**, *21*, 151.

(7) (a) Vlcek, A. A. *Coord. Chem. Rev.* **1982**, *43*, 39. (b) Krejcik, M.; Vlcek, A. A. *Inorg. Chem.* **1992**, *31*, 2390.

(8) DeArmond, M. K.; Hanck, K. W.; Wertz, D. W. *Coord. Chem. Rev.* **1985**, *64*, 65.

(9) (a) Ghosh, P.; Chakravorty, A. *Inorg. Chem.* **1984**, *23*, 2242. (b) Dodsworth, E. S.; Lever, A. B. P. *Chem. Phys. Lett.* **1986**, *124*, 152. (c) Goswami, S.; Mukherjee, R. N.; Chakravorty, A. *Inorg. Chem.* **1983**, *22*, 2825.

(10) Hitoshi, M.; Lever, A. B. P.; Dodsworth, E. S. *Inorg. Chem.* **1993**, *32*, 258 and references therein.

(11) Chlistunoff, J. B.; Bard, A. J. *Inorg. Chem.* **1993**, *32*, 3521.

(12) Braterman, P. S.; Song, J.-I.; Wimmer, F. M.; Wimmer, S.; Kaim, W.; Klein, A.; Peacock, R. D. *Inorg. Chem.* **1992**, *31*, 5084.

(13) (a) Malatesta, L.; Pizzoti, R. *Gazz. Chim. Ital.* **1946**, *76*, 41. (b) Hunter, L.; Roberts, C. B. *J. Chem. Soc.* **1941**, 823. (c) Bamberger, E.; Pemsel, W. *Ber. Dtsch. Chem. Ges.* **1903**, *36*, 85.

0020-1669/94/1333-6140$04.50/0

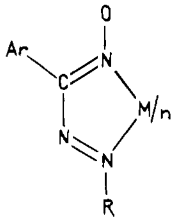

Structure 1

1, with potassium tetrachloroplatinate affording the green

$$PtCl_4^{2-} + 2Hpbo + 2OH^- \rightarrow trans\text{-}Pt(pbo)_2 + 2H_2O + 4Cl^- \quad (1)$$

complex, Pt(pbo)$_2$. It is a normal trans planar bis chelate of bivalent platinum. It, however, has the special property of undergoing quantitative one-electron reduction which can be achieved by exhaustive electrolysis in dichloromethane–acetonitrile solution. Upon addition of 1 equiv of acid (proton) to the reduced solution a dark colored solid having virtually the same chemical composition as that of the parent complex is isolated in excellent yields. The reduced complex actually is *cis*-Pt(pbo)(Hpbo) and its formation can be represented by the stereodynamic electroprotic[16] reaction of eq 2. The reaction of

$$trans\text{-}Pt(pbo)_2 + e + H^+ \rightarrow cis\text{-}Pt(pbo)(Hpbo) \quad (2)$$

eq 2 can also be achieved chemically by treating *trans*-Pt(pbo)$_2$ with ascorbic acid or acidified ethanol.

Both the complexes are diamagnetic in the crystalline state and X-ray work has revealed the trans and cis complexes to be, respectively, monomeric and dimeric in the crystal lattice. The cis complex shows a strong stretching mode in IR at 2920 cm^{-1} which is absent in *trans*-Pt(pbo)$_2$—both complexes show aromatic C–H stretches around 3030 cm^{-1}. The 2920 cm^{-1} band is tentatively assigned to ν_{OH} of the protonated oxime function which is present only in cis complex in an unsymmetrically hydrogen-bonded form as proven by X-ray work.

B. Crystal and Molecular Structure. a. Geometrical Features. The X-ray structures of both the complexes have been determined. Perspective molecular views are shown in Figures 1 and 2 and selected bond parameters are listed in Tables 1 and 2.

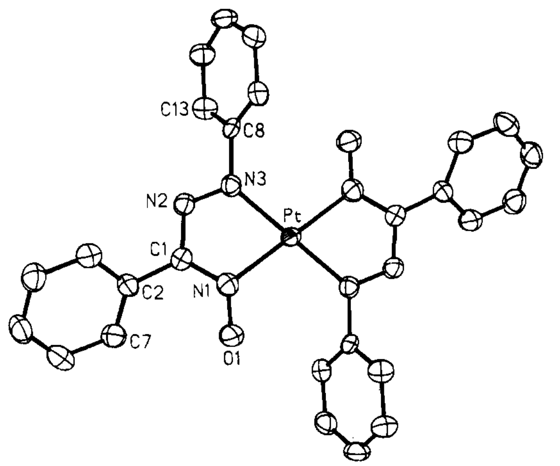

Figure 1. ORTEP plot and atom-labeling scheme for [*cis*-Pt(pbo)(Hpbo)]$_2$. All non-hydrogen atoms are represented by their 40% probability ellipsoids.

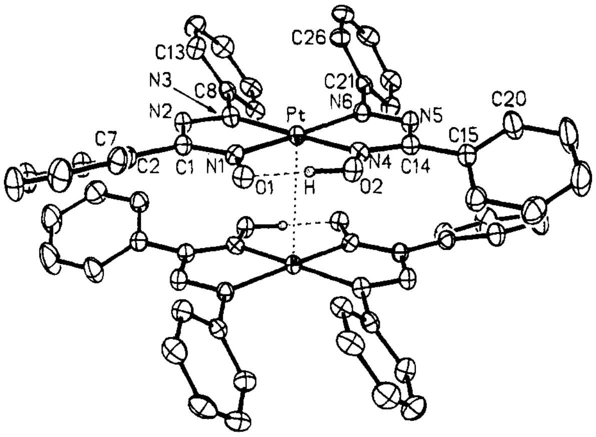

Figure 2. ORTEP plot and atom-labeling scheme for *trans*-Pt(pbo)$_2$. All non-hydrogen atoms are represented by their 40% probability ellipsoids.

Table 1. Selected Bond Distances (Å) and Angles (deg) and Their Estimated Standard Deviations for *trans*-Pt(pbo)$_2$

	Distances		
Pt–N(1)	2.023(5)	Pt–N(3)	2.006(5)
N(2)–C(1)	1.364(9)	N(3)–N(2)	1.275(7)
C(1)–N(1)	1.327(10)	O(1)–N(1)	1.269(9)
	Angles		
N(3)–Pt–N(1)	76.1(3)	N(3)–Pt–N(1A)	103.9(3)
Pt–N(1)–C(1)	114.8(5)	Pt–N(1)–O(1)	122.5(5)
Pt–N(3)–N(2)	118.2(4)	N(1)–Pt–N(1A)	180.0(1)
N(3)–Pt–N(3A)	180.0(1)	N(2)–C(1)–N(1)	115.9(6)
N(3)–N(2)–C(1)	115.0(5)		

The Pt(pbo)$_2$ complex has centrosymmetric trans geometry, the metal atom lying at a crystallographic inversion center. The lattice consists of discrete molecules and there are no unusual intermolecular atomic contacts (the shortest separation between metal atoms being 5.646 Å). The two chelate rings and the oximato oxygen atoms all lie on a plane with mean deviation of ~0.01 Å. The *C*-Ph and *N*-Ph phenyl rings make dihedral angles of 28.8° and 68.9°, respectively, with the above plane.

The reduced complex, Pt(pbo)(Hpbo), occurs as a centrosymmetric dimer in the lattice, the midpoint of the Pt–Pt motif coinciding with a crystallographic inversion center. The coordination sphere of each monomer has cis configuration and the four nitrogen atoms in the PtN$_4$ fragment form a nearly

---

(14) (a) Manivannan, V.; Dutta, S.; Basu, P.; Chakravorty, A. *Inorg. Chem.* **1993**, *32*, 4807. (b) Basu, P.; Pal, S.; Chakravorty, A. *J. Chem. Soc., Dalton Trans.* **1991**, 3217. (c) Chattopadhyay, S.; Basu, P.; Pal, S.; Chakravorty, A. *J. Chem. Soc., Dalton Trans.* **1990**, 3829. (d) Basu, P.; Pal, S.; Chakravorty, A. *Inorg. Chem.* **1988**, *27*, 1848. (e) Pal, S.; Chakravorty, A. *Inorg. Chem.* **1987**, *26*, 4331. (f) Ghosh, B. K.; Mukherjee, R. N.; Chakravorty, A. *Inorg. Chem.* **1987**, *26*, 1946. (g) Pal, S.; Mukherjee, R. N.; Tomas, M.; Falvello, L. R.; Chakravorty, A. *Inorg. Chem.* **1986**, *25*, 200. (h) Pal, S.; Melton, T.; Mukherjee, R. N.; Chakravarty, A. R.; Tomas, M.; Falvello, L. R.; Chakravorty, A. *Inorg. Chem.* **1985**, *24*, 1250. (i) Pal, S.; Bandyopadhyay, D.; Datta, D.; Chakravorty, A. *J. Chem. Soc., Dalton Trans.* **1985**, 159. (j) Bandyopadhyay, D.; Bandyopadhyay, P.; Chakravorty, A.; Cotton, F. A.; Falvello, L. R. *Inorg. Chem.* **1984**, *23*, 1785. (k) Bandyopadhyay, P.; Bandyopadhyay, D.; Chakravorty, A.; Cotton, F. A.; Falvello, L. R.; Han, S. *J. Am. Chem. Soc.* **1983**, 6327. (l) Bandyopadhyay, P.; Mascharak, P. K.; Chakravorty, A. *J. Chem. Soc., Dalton Trans.* **1982**, 675. (m) Bandyopadhyay, P.; Mascharak, P. K.; Chakravorty, A. *J. Chem. Soc., Dalton Trans.* **1981**, 623. (n) Mascharak, P.; Chakravorty, A. *J. Chem. Soc., Dalton Trans.* **1980**, 1698. (o) Kalia, K. C.; Chakravorty, A. *Inorg. Chem.* **1969**, *8*, 2586. (p) Kalia, K. C.; Chakravorty, A. *Inorg. Chem.* **1968**, *7*, 2016.

(15) (a) Chakravarty, A. R.; Chakravorty, A.; Cotton, F. A.; Falvello, L. R.; Ghosh, B. K.; Tomas, M. *Inorg. Chem.* **1983**, 22, 1892. (b) Chakravarty, A. R.; Chakravorty, A. *J. Chem. Soc., Dalton Trans.* **1983**, 961. (c) Chakravarty, A. R.; Chakravorty, A. *Inorg. Chem.* **1981**, *20*, 3138.

(16) (a) Chakravorty, A. *Comments Inorg. Chem. Part A* **1985**, *IV*, 1. (b) Ghosh, P.; Chakravorty, A. *Inorg. Chem.* **1984**, *23*, 2242.

(17) Bandyopadhyay, D.; Bandyopadhyay, P.; Chakravorty, A.; Cotton, F. A.; Falvello, L. R. *Inorg. Chem.* **1983**, 22, 1315.

Table 2. Selected Bond Distances (Å) and Angles (deg) and Their Estimated Standard Deviations for [*cis*-Pt(pbo)(Hpbo)]$_2$

	Distances		
Pt−N(1)	1.962(3)	Pt−N(4)	1.954(3)
Pt−N(3)	2.002(3)	Pt−N(6)	2.002(3)
N(1)−C(1)	1.331(5)	N(4)−C(14)	1.325(5)
N(2)−C(1)	1.376(5)	N(5)−C(14)	1.373(5)
N(2)−N(3)	1.311(5)	N(5)−N(6)	1.306(5)
O(1)−N(1)	1.338(4)	O(2)−N(4)	1.344(4)
Pt−PtA	3.235(1)	O(2)−H	0.98(1)
O(1)···H	1.51(1)		
	Angles		
N(1)−Pt−N(3)	76.6(1)	N(4)−Pt−N(6)	76.0(1)
Pt−N(1)−C(1)	117.6(3)	Pt−N(4)−C(14)	118.1(3)
Pt−N(3)−N(2)	117.5(2)	Pt−N(6)−N(5)	117.7(3)
N(3)−Pt−N(6)	110.0(1)	N(1)−Pt−N(4)	96.9(1)
Pt−N(1)−O(1)	121.6(2)	Pt−N(4)−O(2)	122.3(2)
Pt−N(3)−C(8)	130.3(3)	Pt−N(6)−C(21)	129.9(2)
Pt−N(4)−O(2)	122.3(2)	N(3)−Pt−N(4)	172.2(1)
N(1)−Pt−N(6)	171.2(1)	N(1)−C(1)−N(2)	114.6(3)
N(4)−C(14)−N(5)	114.3(3)	N(3)−N(2)−C(1)	113.6(3)
N(6)−N(5)−C(14)	113.4(3)	N(4)−O(2)−H	99.3(2)

perfect plane from which the metal atom is displaced by 0.088 Å toward the second platinum atom of the dimer. All individual chelate rings of the complex are good planes with mean deviation of ~0.02 Å. The dihedral angle between phenyl rings of the two cis NPh groups is 10.1° and those of the N(3)Ph and N(6)Ph phenyl rings with chelate rings to which they are attached are 49.0° and 58.5°, respectively.

b. Bond Parameters. There are numerous planar platinum(II) compounds that display linear-chain stacking in the crystalline state, the Pt···Pt contacts lying in the range 3.0−3.5 Å.[18] Discrete dimeric complexes incorporating intermetal bridging ligands with Pt···Pt contacts of ~3 Å are also well-documented.[19,20] The [*cis*-Pt(pbo)(Hpbo)]$_2$ complex is unique in being a discrete dimer as opposed to an infinite linear-chain stack even though it is unsupported by bridging ligands. As is implicit in the Pt···Pt length, 3.235(1) Å, the intradimer binding is weak compared to that in bridged dimers. In solution, [*cis*-Pt(pbo)(Hpbo)]$_2$ reversibly dissociates affording monomers, see below.

Many of the hydrogen atoms in [*cis*-Pt(pbo)(Hpbo)]$_2$ were directly observable in difference Fourier maps and one of these was the undissociated oxime hydrogen atom. It lies unsymmetrically between the two oximato oxygen atoms: O(1)···O(2), 2.490(4) Å; O(1)···H, 1.51 Å; H−O(2), 0.98 Å and angle O(1)···H−O(2), 178.1°. Systems with O···H−O bridges spanning the ranges O···O, 2.45−2.65 Å, O···H, 1.39−1.61 Å, and H−O, 0.98−1.09 Å have been documented.[21] We also note that the *cis*-Ru(pbo)(Hpbo) fragment having a hydrogen-bonding situation very similar to that in the platinum complex has been recently identified.[22]

The five-membered chelates have nearly the same bite angles (~76°) in both the trans and the cis complex. However, the other two angles at the metal center between the cis-coordinated pair of atoms vary widely. In *trans*-Pt(pbo)$_2$ they are equal by symmetry and the value is 103.9(3)°. In [*cis*-Pt(pbo)(Hpbo)]$_2$ the N(1)−Pt−N(4) angle occuring in the hydrogen bridged six-membered chelate ring is 96.9(1)° and the angle N(3)−Pt−N(6) opposite to it is 110.0(1)°. This inequality represents a balance between two opposing factors: contraction due to the nearly linear O···H−O bridging, and expansion due to cis phenyl repulsion.

The N−O and Pt−N(oxime) distances in *trans*-Pt(pbo)$_2$, 1.269(9) and 2.023(5) Å, respectively, are normal for a fully deprotonated oxime complex.[23,24] In O···H−O bridged species the above distances are expected to lie in the ranges 1.34−1.40 and 1.95−1.98 Å, respectively[21,23,25] as they do in [*cis*-Pt(pbo)(Hpbo)]$_2$ (Table 2). In the five-membered chelate rings the average N=N length is longer (by 0.03 Å) in cis complex as compared to that in the trans complex. The significance of this will be considered later in this work.

C. Solution Studies. a. Reversible Dissociation of Cis Dimer. The crystalline cis complex is diamagnetic and EPR-inactive. However, dichloromethane solutions are paramagnetic and display an EPR signal with $g = 1.987$. The signal intensity decreases progressively with decreasing temperature (Figure 3). The phenomenon is reversible and upon warming the original intensity is restored. The width of the EPR signal is insensitive to temperature, the separation between the two turnover points remaining constant at 25 ± 2 G in the temperature interval 210−300 K.

The change in the intensity of the signal is evidently due to a temperature-dependent change in the concentration of the paramagnetic species. This is also consistent with variable temperature solution magnetic moment data. The results are in agreement with the equilibrium of eq 3 which corresponds

$$\underset{s=0}{[\textit{cis}\text{-Pt(pbo)(Hpbo)}]_2} \rightarrow \underset{s={}^1/_2}{2\ \textit{cis}\text{-Pt(pbo)(Hpbo)}} \tag{3}$$

to reversible dissociation of the diamagnetic dimer into paramagnetic monomers. The extent of dissociation increases with temperature. Equilibrium constants (K_d) were calculated both from bulk susceptibility and EPR intensity data, and they agree satisfactorily (Table 3). The magnetic moment rises to 1.7 μ_B near 300 K showing that dissociation is virtually complete at room temperature. On the other hand, frozen glasses (77 K) are EPR-inactive. Only dimers are present in this state.

In order to determine the enthalpy and entropy changes (ΔH and ΔS) characterizing the equilibrium process, $-\log K_d$ was plotted against T^{-1} affording a satisfactory straight line with a correlation constant of 0.98 (Figure 3). The enthalpy (ΔH) and entropy (ΔS) parameters were calculated from the slope and intercept of the line with the help of eq 4. The values of ΔH

$$-\log K_d = (1/2.303R)[\Delta H/T - \Delta S] \tag{4}$$

and ΔS are respectively 8.3(±2) kcal mol^{-1} and 23.5(±5) cal mol^{-1} K^{-1}. Both parameters have a positive sign consistent with dissociation. The small ΔH value is a good indication that intradimer binding is weak.

b. Electrochemistry. The unpaired electron in the cis monomer can be ionized electrochemically. In 1:1 dichloromethane−acetonitrile solution (0.1 M in TEAP) at 300 K it displays a quasireversible one-electron cyclic voltammetric response, eq 5, with $E_{1/2}$, 0.52 V (all potentials are referenced

---

(18) (a) Thomas, T. W.; Underhill, A. E. *Chem. Soc. Rev.* **1972**, *1*, 99. (b) Miller, J. S., Ed. *Extended Linear Chain Compounds*; Plenum Press: New York, 1982. (c) Mishowski, V. M.; Houlding, V. H. *Inorg. Chem.* **1991**, *30*, 4446.

(19) (a) Faggiani, R.; Lippert, B.; Lock, C. J. L.; Speranzini, R. A. *J. Am. Chem. Soc.* **1981**, *103*, 1111. (b) Hollis, L. S.; Lippard, S. J. *J. Am. Chem. Soc.* **1981**, *103*, 1231.

(20) (a) Marsh, R. E.; Herbstein, F. H. *Acta Crystallogr.* **1983**, *B39*, 280. (b) Filomena Dos Remedios Pinto, M. A.; Sadler, P. J.; Neidle, S.; Sanderson, M. R.; Subbaiah, A.; Kuroda, R. J. *J. Chem. Soc., Chem. Commun.* **1980**, 13.

(21) Schlemper, E. O. *Acta Crystallogr.* **1977**, *B33*, 2482.

(22) Manivannan, V.; Pal, C. K.; Chattopadhyay, S.; Chakravorty, A. Unpublished results.

(23) Phelps, D. W.; Little, W. F.; Hodgson, D. J. *Inorg. Chem.* **1976**, *15*, 2263.

(24) Chakravorty, A. *Coord. Chem. Rev.* **1974**, *13*, 1.

(25) Hussain, M. S.; Salinas, B. E. V.; Schlemper, E. O. *Acta Crystallogr.* **1979**, *B35*, 628.

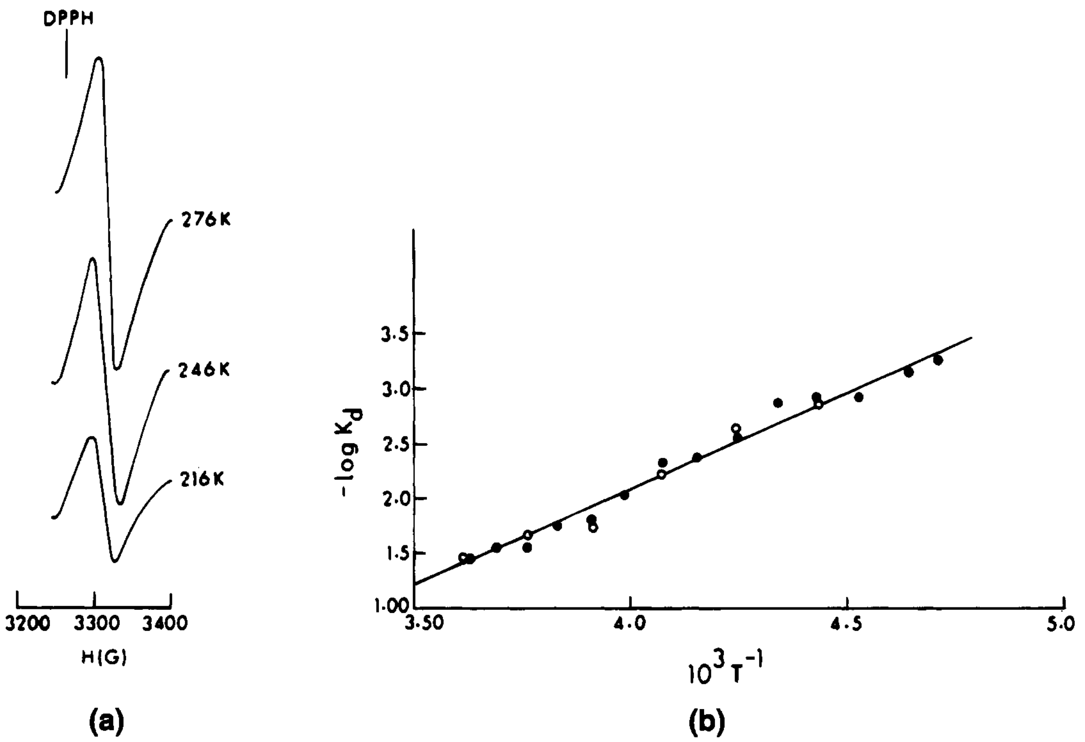

Figure 3. (a) Variable temperature EPR spectra of the cis complex in dichloromethane solution. (b) Plot of $-\log K_d$ vs T^{-1} (●, from EPR; ○, from NMR).

Table 3. Variable Temperature Equilibrium Constants for *cis*-Pt(pbo)(Hpbo)[a,b]

temp, K	10^3K_d, M	temp, K	10^3K_d, M	ΔH, kcal mol^{-1}	ΔS, cal mol^{-1} K^{-1}
216	0.62	256	15.03, 15.47[c]		
226	1.09	266	25.76		
236	2.44, 2.11[c]	276	32.12, 31.60[c]	8.3(±2)	23.5(±5)
246	4.35, 5.03[c]				

[a] Unless otherwise mentioned, data refers to EPR measurements. [b] Concentration of solutions are given in the Experimental Section. [c] From NMR measurements.

to SCE) and peak-to-peak separation, 80 mV. Upon exhaustive

$$cis\text{-Pt(pbo)(Hpbo)}^+ + e \rightarrow cis\text{-Pt(pbo)(Hpbo)} \qquad (5)$$

$$cis\text{-Pt(pbo)(Hpbo)}^+ \rightarrow trans\text{-Pt(pbo)}_2 + H^+ \qquad (6)$$

oxidation at +0.70V, one electron is liberated. The oxidized solution is EPR-inactive as expected but cyclic voltammetry reveals that it contains *cis*-Pt(pbo)(Hpbo)$^+$ ($E_{1/2}$, 0.52 V) mixed with a significant amount of *trans*-Pt(pbo)$_2$ ($E_{1/2}$, −0.28 V, see below). Thus oxidation of the cis complex is attended with partial deprotonation and isomerization, eq 6. Upon adding base (NEt$_3$) to the oxidized solution, conversion to *trans*-Pt(pbo)$_2$ becomes complete.

The *trans*-Pt(pbo)$_2$ complex is also electroactive. The one-electron couple of eq 7 observed cyclic voltammetrically has $E_{1/2}$ of −0.28 V and peak-to-peak separation of 90 mV. Upon electrolysis at −0.5 V one electron is consumed. The reduced solution is EPR-active and is found to contain both *trans*-Pt(pbo)$_2^-$ ($E_{1/2}$, −0.28 V) and *cis*-Pt(pbo)(Hpbo) ($E_{1/2}$, 0.52 V).

$$trans\text{-Pt(pbo)}_2 + e \rightarrow trans\text{-Pt(pbo)}_2^- \qquad (7)$$

$$trans\text{-Pt(pbo)}_2^- + H^+ \rightarrow cis\text{-Pt(pbo)(Hpbo)} \qquad (8)$$

In the formation of the latter, eq 8, the source of proton is unclear: it could be the traces of water present in the solvent/supporting electrolyte or the latter themselves. When a source of proton (acid) is externally added, full conversion to *cis*-Pt(pbo)(Hpbo) occurs and this constitutes an efficient synthetic route for the cis complex, eq 1.

We thus have here a fascinating situation where the interconversion, eq 9, of trans and cis geometries is controlled by

$$trans\text{-Pt(pbo)}_2 \underset{-e,+base}{\overset{+e,+acid}{\rightleftharpoons}} cis\text{-Pt(pbo)(Hpbo)} \qquad (9)$$

ligand-based electroprotic transfer.[16] The trans anion radical (eq 7) has high proton affinity and once protonated transformation to cis geometry having the advantage of O--H−O bridging follows. On the other hand the cis cation (eq 6) tends to lose the proton and upon proton loss, transformation to the sterically more favorable trans form becomes facile.

D. Electronic Structure. In order to have an insight into the nature of the spin-bearing orbital in the cis monomer and intradimer binding in the dimer, MO calculations have been performed in the framework of extended Hückel formalism. For computational convenience the hypothetical model complexes **2** of C_s symmetry and **3** of C_i symmetry have been utilized in

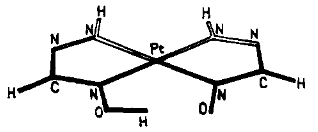

Structure 2

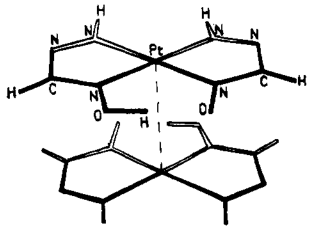

Structure 3

lieu of the actual cis monomer and dimer. The relevant part of the energy level diagram is shown in Figure 4 and orbital compositions of **2** are set out in Table 4.

In **2** the HOMO is the 3A″ orbital with a large azo-π* character and a relatively small contribution from the imine

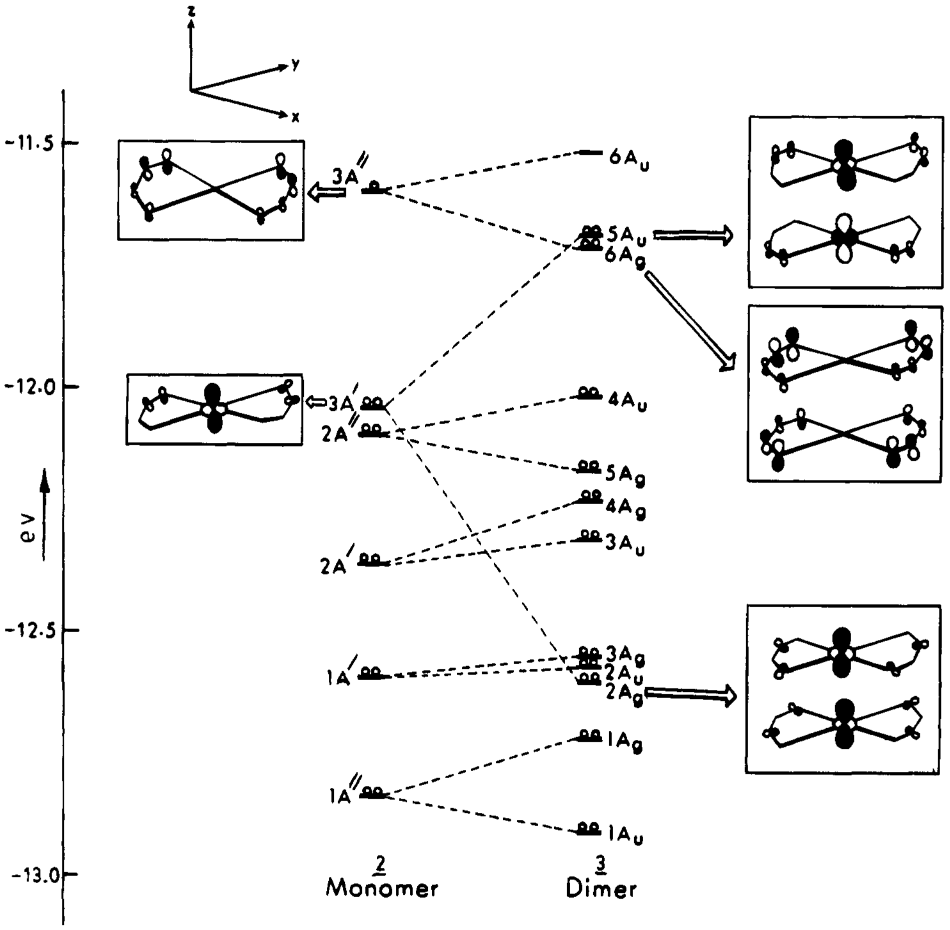

Figure 4. Selected EHMO levels of 2 and 3.

Table 4. Relative Percent Atomic Contributions[a] to the MO's of 2

MO	eigenvalue, eV	Pt	$2N^1$ $(-N^2{=}N^1-Pt)$	$2N^2$ $(-N^2{=}N^1-Pt)$	2C (C=NO)	2N (C=NO)	2O (C=NO)	largest contributor
3A″	−11.60	–	44	30	5	16	4	azo-π^*
3A′	−12.05	80	6	6	–	–	–	d_{z^2}
2A″	−12.10	68	3	5	7	13	3	d_{xz},d_{yz}
2A′	−12.37	82	2	2	–	4	–	d_{xy}
1A′	−12.60	20	15	36	–	14	8	azo lone pair
1A″	−12.85	54	17	13	13	–	–	d_{xz},d_{yz}

[a] These do not add up to 100%, since <1% contributions are not listed.

function. There is no metal contribution in this orbital which is singly occupied in **2**. The unpaired electron in **2** is thus dominantly azo-π^* in nature. Below 3A″ lies 3A′, the filled metal d_{z^2} orbital.

In the dimer the two 3A″ monomer orbitals interact affording the bonding and antibonding combinations 6A$_g$ and 6A$_u$, respectively. Slightly above 6A$_g$ lies 5A$_u$, the antibonding combination of two 3A′ (d_{z^2}) orbitals. The corresponding bonding combination is 2A$_g$. The unpaired electrons of the two monomers get paired up in 6A$_g$ which lies just below the HOMO(5A$_u$). The LUMO is 6A$_u$.

Thus the monomer azo-π^* orbitals (3A″) contribute significantly to the bonding process in the dimer. The d_{z^2} (3A′) interaction also contributes by virtue of its overall bonding nature (bonding character of 2A$_g$ more than offsets the antibonding character of 5A$_u$) which comes via mixing with other terms. Sizable d_{z^2} interaction of this type is a characteristic feature of face-to-face d^8 dimers.[26]

E. Match with Experiments. Some experimental findings can now be rationalized on the basis of the EHMO results. In **4** and **5** the average C=N, C—N, and N=N lengths in the five-membered chelate rings of [*cis*-Pt(pbo)(Hpbo)]$_2$ and *trans*-Pt(pbo)$_2$ are compared. The trans complex is taken as a control

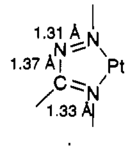

cis
structure **4**

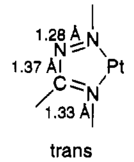

trans
structure **5**

in which azo-π^* orbitals are empty.[27] Whereas the corresponding C=N and C—N lengths are virtually equal in the two rings, the N=N length is 0.03 Å longer in the cis complex. In the model dimer **3**, the filled 6A$_g$ orbital (Figure 4, Table 4) has

---

[26] (a) Smith, D. C.; Gray, H. B. *Coord. Chem. Rev.* **1990**, *100*, 169. (b) Roundhill, D. M.; Gray, H. B. *Acc. Chem. Res.* **1989**, *22*, 55.

[27] We have performed[22] EHMO calculations on the model (i.e., Ph replaced by H, point group C_{2h}) corresponding to *trans*-Pt(pbo)$_2$ and here the LUMO (A$_u$) is a predominantly azo-π^* orbital.

large azo-π^* character with relatively small contributions from the imine function. A selective lengthening of the N═N length is thus anticipated in the cis dimer.

The solution EPR signal (g = 1.987) of the cis monomer does not have any ^{195}Pt hyperfine structure (Figure 3). Thus metal character of the unpaired electron, if any, is small. Extending the EHMO results of **2** (Figure 4, Table 4) we propose that the electron is in an azoimine orbital with large azo-π^* character. The EPR spectra do not show ^{14}N splitting but this could be anticipated. The azo ^{14}N coupling is relatively small (4.8 G) and it is difficult to resolve it due to dominant anisotropic contributions. This has been repeatedly documented in literature.[28]

In the one-electron electrochemical oxidation of *cis*-Pt(pbo)(Hpbo), eq 5, it is evidently the idealized 3A″ electron that is ionized. The complex also displays a quasireversible one-electron reduction ($E_{1/2}$, −0.14 V) and this possibly corresponds to the filling up of the 3A″ orbital. The observed reduction of the trans complex at $E_{1/2}$, −0.28 V is ascribed to electron transfer to the empty azo-π^* orbital.[27]

The *cis*-Pt(pbo)(Hpbo) monomer is essentially an one-electron free radical that is indefinitely stable in solution in air under ambient conditions. The relatively high $E_{1/2}$ value (0.52 V) is no doubt a very important factor contributing to the stability. One major reason for the high $E_{1/2}$ value is the presence of the oximato proton[16] which confers electroneutrality and is itself stabilized by O⋯H−O bridging. Indeed the $E_{1/2}$ values of the couples of eq 5 and 7 differ by a remarkable 0.8 V. Part of this difference could be due to the geometrical change[29] but the main contributor is believed to be the dissimilar states of protonation.

F. Previous Work Revisited. Some years ago the isolation and structural characterization of two bis complexes of bivalent platinum derived from (phenylazo)acetaldoxime, PhN═NC(Me)NOH (abbreviated here as Hpao) were reported. These were formulated as isomers: *trans*-Pt(pao)$_2$ and *cis*-Pt(pao)$_2$.[17,30] The present work does not raise any new question about the trans complex. The cis complex, however, has to be reformulated.

Properties of "cis-Pt(pao)$_2$" have been found to be qualitatively similar to those of the cis complex reported in the present work. It is diamagnetic in the crystalline state which consists of centrosymmetric dimers (Pt⋯Pt, 3.151(1) Å).[17,31] In dichloromethane solution paramagnetic monomers are found to be formed giving rise to an EPR signal (g = 1.976) which is very similar in shape to that of *cis*-Pt(pbo)(Hpbo). Variable temperature studies have confirmed that an equilibrium analogous to that of eq 3 exists but the extent of dissociation is significantly smaller here than in the case of [*cis*-Pt(pbo)(Hpbo)]$_2$.[22] The *trans*-Pt(pao)$_2$ and "cis-Pt(pao)$_2$" complexes are also found to undergo electroprotic processes similar to those in eq 5−8, the corresponding $E_{1/2}$ values being 0.43 V (eq 5 analog) and −0.27 V (eq 7 analog).

It is clear that the correct formulation of "cis-Pt(pao)$_2$" is *cis*-Pt(pao)(Hpao). In the earlier work[17] the presence of the Hpao hydrogen atom was not anticipated and it was not searched for. We first suspected its presence when the synthetic method of eq 1 was devised and the variable temperature solution magnetic and EPR studies were completed.

G. Concluding Remarks. The main findings of this work will now be summarized. It is demonstrated that (phenylazo)benzaldoxime, Hbpo, binds bivalent platinum as a bidentate bis chelating N,N ligand in two different modes. The first mode, pbo$^-$, is expressed in the diamagnetic trans planar complex, *trans*-Pt(pbo)$_2$. The second mode occurs in *cis*-Pt(pbo)(Hpbo) where the bis ligand frame is a dianionic monoradical. The complex is paramagnetic ($s = {}^1/_2$) and in solution it exists in equilibrium with a diamagnetic dimer, [*cis*-Pt(pbo)(Hpbo)]$_2$. The centrosymmetric dimer (Pt⋯Pt, 3.235(1) Å) alone is present in the crystalline state. It is unsupported by any bridging ligand, and O⋯H−O binding occurs within each monomer.

Model EHMO studies have been made on the cis monomer and dimer. The unpaired electron in the monomer belongs to an azoimine orbital with large azo-π^* character but with little or no metal character. In the dimer the interaction between two such monomer ligand orbitals and between two metal d_{z^2} orbitals are important contributors to the bonding process. The EPR spectrum of the monomer and the average N═N length in the dimer are qualitatively consistent with this description.

One-electron electrochemical reduction of *trans*-Pt(pbo)$_2$ affords a reduced complex having high proton affinity and upon addition of acid *cis*-Pt(pbo)(Hpbo) is formed, O⋯H−O bridging being the probable driving force for the geometrical change. Conversely, the *cis*-Pt(pbo)(Hpbo) complex can be electrochemically oxidized liberating one electron, the oxidized complex being prone to proton loss. When base is added the sterically favorable *trans*-Pt(pbo)$_2$ complex is regenerated.

The *trans*-Pt(pbo)$_2$, *cis*-Pt(pbo)(Hpbo), and [*cis*-Pt(pbo)(Hpbo)]$_2$ complexes represent a fascinating triad where geometrical change at the metal site is coupled to proton transfer at the oximato site and electron transfer at the azo site. The combination of azo oxime functions forms the chemical basis of the phenomena observed which do not appear to have any precedence in platinum chemistry. The cis monomer is essentially a planar free radical unaffected by air, the relatively high reduction potential being a factor contributing to this stability. Evidently the chemical or physical binding of this radical to other molecules would be of considerable interest.

A complex of (phenylazo)acetaldoxime(Hpao) earlier described as "cis-Pt(pao)$_2$" has been reformulated as *cis*-Pt(pao)(Hpao). Its behavior is parallel to that of *cis*-Pt(pbo)(Hpbo).

Experimental Section

Materials. Potassium tetrachloroplatinate[32] and (phenylazo)benzaldoxime[33] were prepared by reported methods. Solvents and supporting electrolyte (tetraethylammonium perchlorate, TEAP) for electrochemical work were obtained as before.[34]

Physical Measurements. IR spectra were recorded with a Perkin-Elmer 783 IR spectrophotometer. A Perkin-Elmer 240C elemental analyzer was used to collect microanalytical data (CHN). EPR spectra were recorded at X-band on a Varian E-109C spectrometer equipped with a gas-flow temperature controller for variable-temperature studies.

---

(28) (a) Krejcik, M.; Zalis, S.; Klima, J.; Sykora, D.; Matcheis, W.; Klein, A.; Kaim, W. *Inorg. Chem.* **1993**, *32*, 3362. (b) Kaim, W.; Kohlmann, S. *Inorg. Chem.* **1986**, *25*, 3442. (c) Johnson, C. S.; Chang, R. *J. Chem. Phys.* **1965**, *43*, 3183.

(29) (a) Pramanik, A.; Bag, N.; Ray, D.; Lahiri, G. K.; Chakravorty, A. *Inorg. Chem.* **1991**, *30*, 410. (b) Pramanik, A.; Bag, N.; Chakravorty, A. *J. Chem. Soc., Dalton Trans.* **1993**, 237. (c) Basu, P.; Choudhury, S. B.; Pal, S.; Chakravorty, A. *Inorg. Chem.* **1989**, *28*, 2680. (d) Basu, P.; Chakravorty, A. *Inorg. Chem.* **1992**, *31*, 4980. (e) Bursten, B. E. *J. Am. Chem. Soc.* **1982**, *104*, 1299. (f) Bond, A. M.; Carr, S. W.; Colton, R. *Inorg. Chem.* **1984**, *23*, 2343. (g) Bond, A. M.; Hambley, T. W.; Mann, D. R.; Snow, M. R. *Inorg. Chem.* **1987**, *26*, 2257.

(30) Bandyopadhyay, D.; Bandyopadhyay, P.; Chakravorty, A.; Cotton, F. A.; Falvello, L. R. *Inorg. Chem.* **1984**, *23*, 1785.

(31) The reported weak EPR spectrum in samples of powdered "*cis*-Pt(pao)$_2$" arise from an impurity[17] and is not directly related to the complex.

(32) Livingstone, S. E. *Synth. Inorg. Met.-Org. Chem.* **1971**, *1*, 1.

(33) Kalia, K. C.; Chakravorty, A. *J. Org. Chem.* **1970**, *35*, 2231.

(34) (a) Goswami, S.; Chakravarty, A. R.; Chakravorty, A. *Inorg. Chem.* **1982**, *20*, 2246. (b) Datta, D.; Mascharak, P. K.; Chakravorty, A. *Inorg. Chem.* **1981**, *20*, 1673.

Table 5. Crystallographic Data for *trans*-Pt(pbo)$_2$ and [*cis*-Pt(pbo)(Hpbo)]$_2$

	trans-Pt(pbo)$_2$	[*cis*-Pt(pbo)(Hpbo)]$_2$
empirical formula	$C_{26}H_{20}N_6O_2Pt$	$C_{52}H_{42}N_{12}O_4Pt_2$
fw	643.6	1289.2
space group	$P2_1/n$	$C2/c$
a, Å	5.646(4)	25.183(8)
b, Å	10.784(7)	8.849(4)
c, Å	18.367(14)	20.839(8)
β, deg	98.11(5)	90.09(3)
V, Å^3	1107(1)	4644(3)
Z	2	4
T, K	295	295
λ, Å	0.71073	0.71073
ϱ_{calcd}, g cm^3	1.931	1.844
μ, cm^{-1}	63.76	60.80
transm coeff[a]	0.7731/1	0.7791/1
R,[b] %	2.74	2.42
R_w,[c] %	3.20	2.90
GOF[d]	1.37	1.13

[a] Maximum value normalized to 1. [b] $R = \sum||F_o| - |F_c||/\sum|F_o|$. [c] $R_w = [\sum w(|F_o| - |F_c|)^2/\sum w|F_o|^2]^{1/2}$; $w^{-1} = \sigma^2(|F_o|) + g|F_o|^2$; $g = 0.00020$ for *trans*-Pt(pbo)$_2$ and $g = 0.00025$ for [*cis*-Pt(pbo)(Hpbo)]$_2$. [d] The goodness of fit is defined as $[w(|F_o| - |F_c|)^2/(n_o - n_v)]^{1/2}$ where n_o and n_v denote the numbers of data and variables, respectively.

Table 6. Atomic Coordinates ($\times 10^4$) and Equivalent Isotropic Displacement Coefficients (Å^2 × 10^3) of *trans*-Pt(pbo)$_2$[a]

	x	*y*	*z*	*U*(eq)
Pt	0	0	0	31(1)
O(1)	3653(10)	1076(5)	1094(3)	51(2)
N(1)	2988(9)	87(7)	749(3)	38(1)
N(2)	3197(10)	−1967(5)	469(3)	35(2)
N(3)	1257(9)	−1743(5)	45(3)	30(2)
C(1)	4152(13)	−978(7)	871(4)	34(2)
C(2)	6296(12)	−1185(6)	1426(3)	34(2)
C(3)	6617(14)	−2370(6)	1725(4)	44(2)
C(4)	8656(14)	−2645(7)	2222(4)	49(3)
C(5)	10326(14)	−1738(7)	2425(4)	49(3)
C(6)	10029(14)	−564(8)	2130(4)	46(2)
C(7)	7998(14)	−276(6)	1632(4)	38(2)
C(8)	383(11)	−2805(6)	−398(3)	31(2)
C(9)	−1732(11)	−3367(6)	−278(3)	36(2)
C(10)	−2452(12)	−4444(7)	−651(4)	41(2)
C(11)	−1075(12)	−4908(7)	−1154(3)	43(2)
C(12)	954(13)	−4306(7)	−1295(4)	43(2)
C(13)	1711(12)	−3249(6)	−915(3)	40(2)

[a] Equivalent isotropic *U* defined as one third of the trace of the orthogonalized U_{ij} tensor.

A calibrated copper-constantan thermocouple was used for temperature determination. DPPH ($g = 2.0037$) was used to calibrate the spectra. Solution magnetic moments were determined by the Evans method[35] from the shift of the ^1H signal of CH_2Cl_2 using a Brucker 270-MHz spectrometer fitted with a variable temperature accessory. Coaxial tubes were used for placing pure solvent and solution. Electrochemical measurements were performed on a PAR Model 370-4 electrochemistry system as reported earlier.[36] All potentials reported in this work are referenced to saturated calomel electrode (SCE) and are uncorrected for junction contribution.

Table 7. Atomic Coordinates ($\times 10^4$) and Equivalent Isotropic Displacement Coefficients (Å^2 × 10^3) for [*cis*-Pt(pbo)(Hpbo)]$_2$[a]

	x	*y*	*z*	*U*(eq)
Pt	2458(1)	4299(1)	−127(1)	30(1)
O(1)	2978(1)	3244(3)	−1282(1)	39(1)
O(2)	1990(1)	3314(3)	−1331(1)	40(1)
N(1)	3055(1)	3826(4)	−697(1)	32(1)
N(2)	3562(1)	4790(4)	112(2)	37(1)
N(3)	3095(1)	4934(4)	383(1)	34(1)
N(4)	1891(1)	3769(4)	−728(1)	32(1)
N(5)	1340(1)	4549(4)	64(2)	39(1)
N(6)	1793(1)	4894(4)	333(2)	33(1)
C(1)	3542(2)	4145(5)	−488(2)	35(1)
C(2)	4047(2)	3878(5)	−818(2)	38(1)
C(3)	4509(2)	3737(6)	−445(2)	49(1)
C(4)	4994(2)	3444(7)	−733(3)	67(2)
C(5)	5023(2)	3301(8)	−1389(3)	73(2)
C(6)	4570(2)	3480(7)	−1761(3)	68(2)
C(7)	4086(2)	3787(6)	−1487(2)	47(1)
C(8)	3129(2)	5730(5)	981(2)	35(1)
C(9)	2852(2)	5182(5)	1511(2)	38(1)
C(10)	2893(2)	5937(5)	2091(2)	49(2)
C(11)	3183(2)	7248(6)	2136(2)	55(2)
C(12)	3455(2)	7798(6)	1606(2)	53(2)
C(13)	3434(2)	7022(6)	1028(2)	45(1)
C(14)	1394(2)	3902(5)	−531(2)	35(1)
C(15)	905(2)	3550(5)	−885(2)	39(1)
C(16)	891(2)	2423(5)	−1357(2)	48(2)
C(17)	414(2)	2089(7)	−1652(3)	65(2)
C(18)	−46(2)	2832(9)	−1488(3)	82(2)
C(19)	−26(2)	3957(9)	−1032(4)	94(3)
C(20)	442(2)	4303(6)	−736(3)	63(2)
C(21)	1726(2)	5735(5)	920(2)	33(1)
C(22)	1428(2)	5120(5)	1415(2)	41(1)
C(23)	1374(2)	5963(5)	1981(2)	49(2)
C(24)	1599(2)	7370(5)	2028(2)	53(2)
C(25)	1885(2)	7967(5)	1531(2)	48(1)
C(26)	1953(2)	7149(5)	967(2)	42(1)

[a] Equivalent isotropic *U* defined as one-third of the trace of the orthogonalized U_{ij} tensor.

Preparation of Compounds. *trans*-Bis[(phenylazo)benzaldoximato]platinum(II), *trans*-Pt(pbo)$_2$. To an aqueous solution (25 mL) of K_2PtCl_4 (0.830 g, 2 mmol) was added dropwise with magnetic stirring a solution of (phenylazo)benzaldoxime (0.900 g, 4 mmol) in 40 mL of 0.5 N potassium hydroxide. Stirring was continued for 6 h. The dark colored precipitate was thoroughly washed with water and then with ether. The crude product was chromatographed on a silica gel (60–120 mesh) column using benzene as eluent. The deep green band was collected and evaporated to dryness in air. Recrystallization was done from a dichloromethane–hexane mixture. The yield was 0.88 g (57%). Anal. Calcd for $PtC_{26}H_{20}N_6O_2$: C, 48.52; H, 3.11; N, 13.06. Found: C, 48.70; H, 3.10; N, 13.11.

***cis*-[(Phenylazo)benzaldoximato][(phenylazo)benzaldoxime]-platinum(II) Dimer, [*cis*-Pt(pbo)(Hpbo)]$_2$.** A solution of 30 mg (0.047 mmol) of *trans*-Pt(pbo)$_2$ in 20 mL of acetonitrile–dichloromethane (1:1) mixture (0.1 M TEAP) was reduced coulometrically at a constant potential of −0.5 V vs SCE in dinitrogen atmosphere. Electrolysis stopped when 4.52 C had passed. The calculated one-electron coulomb count is 4.50. To the blue-green solution thus obtained was added 2 mL of 0.025 N $HClO_4$ (in acetonitrile). The brown solution was evaporated under reduced pressure. The solid residue was washed with water and dried over P_4O_{10} and was treated with a mixture of benzene–petroleum ether (4:1) at room temperature. The resulting brown solution was filtered through a sintered frit. The filtrate was evaporated to dryness and chromatographed over a silica gel column prepared in petroleum spirit. A mixture of petroleum spirit–benzene (1:1) was used as the eluent. The brown band was collected and evaporated to dryness. Recrystallization was done from dichloromethane–hexane mixture. The yield was 25 mg (83%). Anal. Calcd for [$PtC_{26}H_{21}N_6O_2$]: C, 48.44; H, 3.26; N, 13.04. Found: C, 48.50; H, 3.22; N, 13.16.

Conversion of [*cis*-Pt(pbo)(Hpbo)]$_2$ to *trans*-Pt(pbo)$_2$. A solution of 24 mg (0.037 mmol) of [*cis*-Pt(pbo)(Hpbo)]$_2$ in 20 mL of acetonitrile–dichloromethane (1:1) mixture (0.1 M TEAP) was oxidized coulometrically at a constant potential of +0.7 V vs SCE in dinitrogen atmosphere. Electrolysis stopped when 3.26 C had passed. The calculated one-electron coulomb count was 3.596. To brown-green solution thus obtained was added 1.4 mL of 0.026 N NEt_3 (in acetonitrile). The solution color immediately changed to deep green. The green solution was evaporated under reduced pressure. The solid residue was washed with water and dried over P_4O_{10} and was treated with a mixture of benzene–petroleum spirit (4:1) at room temperature.

---

(35) Evans, D. F. *J. Chem. Soc.* **1959**, 2003.

(36) Chandra, S. K.; Basu, P.; Ray, D.; Pal, S.; Chakravorty, A. *Inorg. Chem.* **1990**, *29*, 2423.

The resulting solution was filtered through sintered frit. The filtrate was evaporated and chromatographed on silica gel (60−120 mesh) column prepared in benzene. Benzene was used as eluent. The deep green band was collected and upon evaporation of the solvent the green colored *trans*-Pt(pbo)$_2$ yielded 20 mg (83%).

Solution Equilibrium Constants. The dissociation constant, K_d, for the reaction of eq 3 can be written as in eq 10, where X is the total

$$K_d = [\text{monomer}]^2/[\text{dimer}] = 2x^2/(X - x) \qquad (10)$$

solute concentration expressed as monomer and x is the equilibrium concentration of the monomer. The equilibrium concentration of dimer is then $(X - x)/2$. Variable temperature K_d values were determined in dichloromethane solution by EPR and NMR spectroscopy. Concentrations were duly corrected for density change of the solvent with change in temperature. The EPR method ($X = 1.98 \times 10^{-3}$ M at 276 K) essentially involved spin counting (the count is a measure of x in eq 10) made[37] by comparing EPR signal heights with that of a standard crystal of known mass (we used $CuSO_4{\cdot}5H_2O$). In the NMR method ($X = 6.87 \times 10^{-2}$ M at 276 K) magnetic moments (μ_{eff}) of the solute in solution were calculated using the Evans formula.[35] The moments were found as 0.59, 0.72, 0.92, and 1.07 μ_B at 236, 246, 256, and 276 K, respectively. The quantity $(\mu_{eff}/1.73)^2$ is a measure of x in eq 10 ($1.73\mu_B$ corresponds to the case $X = x$).

Molecular Orbital Calculations. Extended Huckel calculations were performed on an IBM PC AT using the ICON software package originally developed by Hoffmann.[38] The atomic parameters and H_{ii} values for C,O,H,N and Pt were taken from literature.[39] The orthogonal coordinate system chosen for the calculations is defined in Figure 4. The averaged experimental bond distance and angles were used in our calculations. The C−H distance was taken as 0.96 Å.

X-ray Structure Determination. Crystals were grown (298 K) by slow diffusion of hexane into dichloromethane solution (crystal size: trans, 0.10 × 0.07 × 0.50 mm^3; cis, 0.15 × 0.14 × 0.44 mm^3). Cell parameters were determined by least square fits of 25 machine centered reflections ($2\theta = 15-30°$). Since the β value (90.09°) of the cis complex lies close to 90°, careful tests (axial photography, Friedel equivalence) were made to ensure that symmetry higher than monoclinic did not exist. Systematic absences afforded the space group $P2_1/n$ for the trans complex. The cis complex could belong either to Cc or $C2/c$—successful structure solution confirmed $C2/c$ space group. Data were collected by ω-scan technique in the range of $2° \leqslant 2\theta \leqslant 55°$ on a Siemens R3m/V diffractometer with Mo Kα radiation monochromated by a graphite crystal. Two check reflections measured after every 98 reflections did not show any significant change in intensity. Data were corrected for Lorentz-polarization effect and absorption (azimuthal scan[40]). Of the 2541 (trans) and 5342 (cis) unique reflections 1553 and 4173 with $I > 3\sigma(I)$ were used for respective structure solution (heavy atom method). All the non-hydrogen atoms were made anisotropic. In the case of the cis complex the hydrogen atoms linked with O2, C3, C4, C7, C9, C12, C13, C16, C18, and C26 were located with difference Fourier maps. The rest of the hydrogen atoms in the cis complex and all the hydrogen atoms in the trans complex were added at calculated positions with fixed U (0.08 Å^2) in the last cycle of refinement. Least square refinements were performed by full matrix procedures. All calculations were done on a MicroVAX II computer with programs of SHELXTL-PLUS.[41] Significant crystal data are listed in Table 5. Atomic coordinates and isotropic thermal parameters were listed in Tables 6 and 7.

Acknowledgment. We are thankful to the Department of Science and Technology, New Delhi, for financial support. The Council of Scientific and Industrial Research provided a fellowship to C.K.P. Affiliation with the Jawaharlal Nehru Centre for Advanced Scientific Research, Bangalore India, is acknowledged. We are thankful to Prof. E. D. Jemmis and Mr. G. Nagasrinivas for helping in the EHMO calculations and to Drs. P. Basu, D. Ray, and R. Bagchi for some preliminary works.

Supplementary Material Available: Tables SI−SVIII, listing anisotropic thermal parameters, complete bond distances and angles, and hydrogen atom positional parameters (6 pages). Ordering information is given on any current masthead page.

---

[37] Poole, C. P. *Electron Spin Resonance. A Comprehensive Treatise on Experimental Techniques*; 2nd ed., Wiley-Interscience: New York, 1983; pp 400−409.

[38] (a) Hoffmann, R. *J. Chem. Phys.* **1963**, *39*, 1397. (b) Ammeter, J. H.; Burgi, H.-B.; Thebeault, J. C.; Hoffmann, R. *J. Am. Chem. Soc.* **1978**, *100*, 3686.

[39] (a) Tatsumi, K.; Hoffmann, R. *J. Am. Chem. Soc.* **1981**, *103*, 3328. (b) Hoffman, D. M.; Hoffmann, R.; Fisel, C. R. *J. Am. Chem. Soc.* **1982**, *104*, 3858.

[40] North, A. C. T.; Phillips, D. C.; Mathews, F. S. *Acta Crystallogr.* **1968**, *A24*, 351.

[41] Sheldrick, G. M. SHELXTL-PLUS 88, Structure Determination Software Programs; Nicolet Instrument Corp.: Madison, WI, 1988.